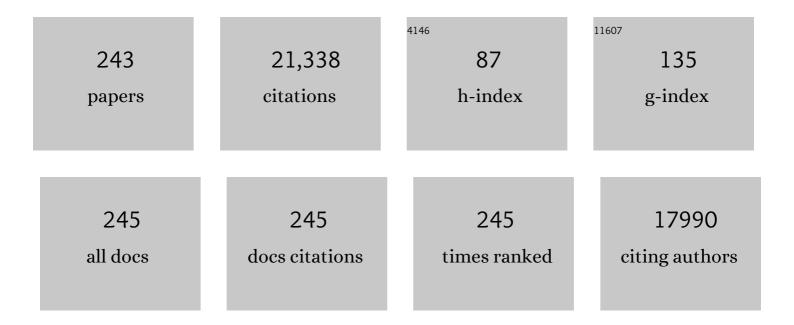
Yaoyu Zhou

List of Publications by Year in descending order

Source: https://exaly.com/author-pdf/6700186/publications.pdf Version: 2024-02-01



#	Article	IF	CITATIONS
1	Modification of biochar derived from sawdust and its application in removal of tetracycline and copper from aqueous solution: Adsorption mechanism and modelling. Bioresource Technology, 2017, 245, 266-273.	9.6	553
2	Insight into highly efficient simultaneous photocatalytic removal of Cr(VI) and 2,4-diclorophenol under visible light irradiation by phosphorus doped porous ultrathin g-C3N4 nanosheets from aqueous media: Performance and reaction mechanism. Applied Catalysis B: Environmental, 2017, 203, 343-354.	20.2	513
3	An overview on engineering the surface area and porosity of biochar. Science of the Total Environment, 2021, 763, 144204.	8.0	434
4	Adsorption of tetracycline antibiotics from aqueous solutions on nanocomposite multi-walled carbon nanotube functionalized MIL-53(Fe) as new adsorbent. Science of the Total Environment, 2018, 627, 235-244.	8.0	418
5	Atomic scale g-C3N4/Bi2WO6 2D/2D heterojunction with enhanced photocatalytic degradation of ibuprofen under visible light irradiation. Applied Catalysis B: Environmental, 2017, 209, 285-294.	20.2	390
6	One-step synthesis of Co-doped UiO-66 nanoparticle with enhanced removal efficiency of tetracycline: Simultaneous adsorption and photocatalysis. Chemical Engineering Journal, 2018, 353, 126-137.	12.7	356
7	Efficacy of carbonaceous nanocomposites for sorbing ionizable antibiotic sulfamethazine from aqueous solution. Water Research, 2016, 95, 103-112.	11.3	326
8	Metal-free carbon materials-catalyzed sulfate radical-based advanced oxidation processes: A review on heterogeneous catalysts and applications. Chemosphere, 2017, 189, 224-238.	8.2	320
9	Plasmonic Bi Metal Deposition and g-C ₃ N ₄ Coating on Bi ₂ WO ₆ Microspheres for Efficient Visible-Light Photocatalysis. ACS Sustainable Chemistry and Engineering, 2017, 5, 1062-1072.	6.7	289
10	Insight into electro-Fenton and photo-Fenton for the degradation of antibiotics: Mechanism study and research gaps. Chemical Engineering Journal, 2018, 347, 379-397.	12.7	287
11	Adsorption of phosphate from aqueous solution using iron-zirconium modified activated carbon nanofiber: Performance and mechanism. Journal of Colloid and Interface Science, 2017, 493, 17-23.	9.4	267
12	Carbon-based materials as adsorbent for antibiotics removal: Mechanisms and influencing factors. Journal of Environmental Management, 2019, 237, 128-138.	7.8	266
13	Arbuscular mycorrhizal fungi-induced mitigation of heavy metal phytotoxicity in metal contaminated soils: A critical review. Journal of Hazardous Materials, 2021, 402, 123919.	12.4	266
14	Iron Containing Metal–Organic Frameworks: Structure, Synthesis, and Applications in Environmental Remediation. ACS Applied Materials & Interfaces, 2017, 9, 20255-20275.	8.0	250
15	Physicochemical features, metal availability and enzyme activity in heavy metal-polluted soil remediated by biochar and compost. Science of the Total Environment, 2020, 701, 134751.	8.0	249
16	Multi-walled carbon nanotube/amino-functionalized MIL-53(Fe) composites: Remarkable adsorptive removal of antibiotics from aqueous solutions. Chemosphere, 2018, 210, 1061-1069.	8.2	241
17	Diagnosis of soil contamination using microbiological indices: A review on heavy metal pollution. Journal of Environmental Management, 2019, 242, 121-130.	7.8	238
18	Construction of plasmonic Ag modified phosphorous-doped ultrathin g-C3N4 nanosheets/BiVO4 photocatalyst with enhanced visible-near-infrared response ability for ciprofloxacin degradation. Journal of Hazardous Materials, 2018, 344, 758-769.	12.4	227

#	Article	IF	CITATIONS
19	Effective removal of Cr(<scp>vi</scp>) using β-cyclodextrin–chitosan modified biochars with adsorption/reduction bifuctional roles. RSC Advances, 2016, 6, 94-104.	3.6	221
20	Synergistic effect of iron doped ordered mesoporous carbon on adsorption-coupled reduction of hexavalent chromium and the relative mechanism study. Chemical Engineering Journal, 2014, 239, 114-122.	12.7	220
21	Microplastics and environmental pollutants: Key interaction and toxicology in aquatic and soil environments. Journal of Hazardous Materials, 2022, 422, 126843.	12.4	220
22	Enhanced photocatalytic degradation of norfloxacin in aqueous Bi2WO6 dispersions containing nonionic surfactant under visible light irradiation. Journal of Hazardous Materials, 2016, 306, 295-304.	12.4	216
23	Current progress in biosensors for heavy metal ions based on DNAzymes/DNA molecules functionalized nanostructures: A review. Sensors and Actuators B: Chemical, 2016, 223, 280-294.	7.8	216
24	Selenium contamination, consequences and remediation techniques in water and soils: A review. Environmental Research, 2018, 164, 288-301.	7.5	215
25	Activation of peroxymonosulfate (PMS) by spinel ferrite and their composites in degradation of organic pollutants: A Review. Chemical Engineering Journal, 2021, 414, 128800.	12.7	211
26	Plasmonic resonance excited dual Z-scheme BiVO ₄ /Ag/Cu ₂ O nanocomposite: synthesis and mechanism for enhanced photocatalytic performance in recalcitrant antibiotic degradation. Environmental Science: Nano, 2017, 4, 1494-1511.	4.3	202
27	Antimony contamination, consequences and removal techniques: A review. Ecotoxicology and Environmental Safety, 2018, 156, 125-134.	6.0	199
28	A sustainable biochar catalyst synergized with copper heteroatoms and CO ₂ for singlet oxygenation and electron transfer routes. Green Chemistry, 2019, 21, 4800-4814.	9.0	188
29	Fabrication of sustainable manganese ferrite modified biochar from vinasse for enhanced adsorption of fluoroquinolone antibiotics: Effects and mechanisms. Science of the Total Environment, 2020, 709, 136079.	8.0	187
30	Insight into the dual-channel charge-charrier transfer path for nonmetal plasmonic tungsten oxide based composites with boosted photocatalytic activity under full-spectrum light. Applied Catalysis B: Environmental, 2018, 235, 225-237.	20.2	184
31	Bioremediation of water containing pesticides by microalgae: Mechanisms, methods, and prospects for future research. Science of the Total Environment, 2020, 707, 136080.	8.0	184
32	Enhancement of Cd(II) adsorption by polyacrylic acid modified magnetic mesoporous carbon. Chemical Engineering Journal, 2015, 259, 153-160.	12.7	182
33	Cu and Co nanoparticles co-doped MIL-101 as a novel adsorbent for efficient removal of tetracycline from aqueous solutions. Science of the Total Environment, 2019, 650, 408-418.	8.0	182
34	Sustainable stabilization/solidification of municipal solid waste incinerator fly ash by incorporation of green materials. Journal of Cleaner Production, 2019, 222, 335-343.	9.3	177
35	Mn-doped zirconium metal-organic framework as an effective adsorbent for removal of tetracycline and Cr(VI) from aqueous solution. Microporous and Mesoporous Materials, 2019, 277, 277-285.	4.4	177
36	Electrocatalytic properties of N-doped graphite felt in electro-Fenton process and degradation mechanism of levofloxacin. Chemosphere, 2017, 182, 306-315.	8.2	176

#	Article	IF	CITATIONS
37	Efficient charge transfer in aluminum-cobalt layered double hydroxide derived from Co-ZIF for enhanced catalytic degradation of tetracycline through peroxymonosulfate activation. Chemical Engineering Journal, 2020, 382, 122802.	12.7	174
38	A visual application of gold nanoparticles: Simple, reliable and sensitive detection of kanamycin based on hydrogen-bonding recognition. Sensors and Actuators B: Chemical, 2017, 243, 946-954.	7.8	170
39	Treatment of arsenic in acid wastewater and river sediment by Fe@Fe2O3 nanobunches: The effect of environmental conditions and reaction mechanism. Water Research, 2017, 117, 175-186.	11.3	169
40	Insight into highly efficient co-removal of p-nitrophenol and lead by nitrogen-functionalized magnetic ordered mesoporous carbon: Performance and modelling. Journal of Hazardous Materials, 2017, 333, 80-87.	12.4	167
41	Applications and factors influencing of the persulfate-based advanced oxidation processes for the remediation of groundwater and soil contaminated with organic compounds. Journal of Hazardous Materials, 2018, 359, 396-407.	12.4	164
42	Facile fabrication of mediator-free Z-scheme photocatalyst of phosphorous-doped ultrathin graphitic carbon nitride nanosheets and bismuth vanadate composites with enhanced tetracycline degradation under visible light. Journal of Colloid and Interface Science, 2018, 509, 219-234.	9.4	160
43	Unique g-C3N4/PDI-g-C3N4 homojunction with synergistic piezo-photocatalytic effect for aquatic contaminant control and H2O2 generation under visible light. Applied Catalysis B: Environmental, 2022, 303, 120929.	20.2	155
44	Construction of Plasmonic Ag and Nitrogen-Doped Graphene Quantum Dots Codecorated Ultrathin Graphitic Carbon Nitride Nanosheet Composites with Enhanced Photocatalytic Activity: Full-Spectrum Response Ability and Mechanism Insight. ACS Applied Materials & Interfaces, 2017, 9, 42816-42828.	8.0	152
45	Advances in enhanced volatile fatty acid production from anaerobic fermentation of waste activated sludge. Science of the Total Environment, 2019, 694, 133741.	8.0	149
46	Synthesis and application of iron and zinc doped biochar for removal of p-nitrophenol in wastewater and assessment of the influence of co-existed Pb(II). Applied Surface Science, 2017, 392, 391-401.	6.1	148
47	pH-dependent degradation of p-nitrophenol by sulfidated nanoscale zerovalent iron under aerobic or anoxic conditions. Journal of Hazardous Materials, 2016, 320, 581-590.	12.4	147
48	Analyses of tetracycline adsorption on alkali-acid modified magnetic biochar: Site energy distribution consideration. Science of the Total Environment, 2019, 650, 2260-2266.	8.0	144
49	Simultaneous removal of lead and phenol contamination from water by nitrogen-functionalized magnetic ordered mesoporous carbon. Chemical Engineering Journal, 2015, 259, 854-864.	12.7	141
50	Facile fabrication of a direct Z-scheme Ag2CrO4/g-C3N4 photocatalyst with enhanced visible light photocatalytic activity. Journal of Molecular Catalysis A, 2016, 421, 209-221.	4.8	141
51	Remediation of Cu, Pb, Zn and Cd-contaminated agricultural soil using a combined red mud and compost amendment. International Biodeterioration and Biodegradation, 2017, 118, 73-81.	3.9	141
52	Responses of bacterial community and functional marker genes of nitrogen cycling to biochar, compost and combined amendments in soil. Applied Microbiology and Biotechnology, 2016, 100, 8583-8591.	3.6	140
53	Appraising growth, oxidative stress and copper phytoextraction potential of flax (Linum) Tj ETQq1 1 0.784314 rg Management, 2020, 257, 109994.	gBT /Overl 7.8	lock 10 Tf 50 136
54	Remediation of persistent organic pollutants in aqueous systems by electrochemical activation of persulfates: A review. Journal of Environmental Management, 2020, 260, 110125.	7.8	136

#	Article	IF	CITATIONS
55	Degradation of sulfamethazine by biochar-supported bimetallic oxide/persulfate system in natural water: Performance and reaction mechanism. Journal of Hazardous Materials, 2020, 398, 122816.	12.4	133
56	Mesoporous carbon nitride based biosensor for highly sensitive and selective analysis of phenol and catechol in compost bioremediation. Biosensors and Bioelectronics, 2014, 61, 519-525.	10.1	132
57	Agricultural biomass/waste as adsorbents for toxic metal decontamination of aqueous solutions. Journal of Molecular Liquids, 2019, 295, 111684.	4.9	131
58	Construction of MIL-53(Fe) metal-organic framework modified by silver phosphate nanoparticles as a novel Z-scheme photocatalyst: Visible-light photocatalytic performance and mechanism investigation. Applied Surface Science, 2019, 465, 103-115.	6.1	129
59	Catalytic reduction–adsorption for removal of p-nitrophenol and its conversion p-aminophenol from water by gold nanoparticles supported on oxidized mesoporous carbon. Journal of Colloid and Interface Science, 2016, 469, 78-85.	9.4	128
60	A sustainable ferromanganese biochar adsorbent for effective levofloxacin removal from aqueous medium. Chemosphere, 2019, 237, 124464.	8.2	127
61	Nanoporous Au-based chronocoulometric aptasensor for amplified detection of Pb2+ using DNAzyme modified with Au nanoparticles. Biosensors and Bioelectronics, 2016, 81, 61-67.	10.1	126
62	Core-shell nanomaterials: Applications in energy storage and conversion. Advances in Colloid and Interface Science, 2019, 267, 26-46.	14.7	125
63	Synergistic adsorption and reduction of hexavalent chromium using highly uniform polyaniline–magnetic mesoporous silica composite. Chemical Engineering Journal, 2014, 254, 302-312.	12.7	124
64	Competitive removal of Cd(<scp>ii</scp>) and Pb(<scp>ii</scp>) by biochars produced from water hyacinths: performance and mechanism. RSC Advances, 2016, 6, 5223-5232.	3.6	124
65	Current progress in the adsorption, transport and biodegradation of antibiotics in soil. Journal of Environmental Management, 2019, 251, 109598.	7.8	123
66	A review of recent applications of porous metals and metal oxide in energy storage, sensing and catalysis. Journal of Materials Science, 2019, 54, 949-973.	3.7	121
67	Cd(II) removal from aqueous solution by adsorption on α-ketoglutaric acid-modified magnetic chitosan. Applied Surface Science, 2014, 292, 710-716.	6.1	120
68	Biochar-based functional materials in the purification of agricultural wastewater: Fabrication, application and future research needs. Chemosphere, 2018, 197, 165-180.	8.2	119
69	Experimental and theoretical aspects of biochar-supported nanoscale zero-valent iron activating H2O2 for ciprofloxacin removal from aqueous solution. Journal of Hazardous Materials, 2019, 380, 120848.	12.4	119
70	Optimizing the synthesis of Fe/Al (Hydr)oxides-Biochars to maximize phosphate removal via response surface model. Journal of Cleaner Production, 2019, 237, 117770.	9.3	119
71	Single and simultaneous adsorption of pefloxacin and Cu(II) ions from aqueous solutions by oxidized multiwalled carbon nanotube. Science of the Total Environment, 2019, 646, 29-36.	8.0	116
72	Current progress in remediation of chlorinated volatile organic compounds: A review. Journal of Industrial and Engineering Chemistry, 2018, 62, 106-119.	5.8	115

#	Article	IF	CITATIONS
73	Cobalt nanoparticles-embedded magnetic ordered mesoporous carbon for highly effective adsorption of rhodamine B. Applied Surface Science, 2014, 314, 746-753.	6.1	114
74	Aptamer-based biosensors for detection of lead(<scp>ii</scp>) ion: a review. Analytical Methods, 2017, 9, 1976-1990.	2.7	114
75	Highly effective adsorption of cationic and anionic dyes on magnetic Fe/Ni nanoparticles doped bimodal mesoporous carbon. Journal of Colloid and Interface Science, 2015, 448, 451-459.	9.4	113
76	A review on nitrogen transformation in hydrochar during hydrothermal carbonization of biomass containing nitrogen. Science of the Total Environment, 2021, 756, 143679.	8.0	108
77	Sustainable biochar/MgFe2O4 adsorbent for levofloxacin removal: Adsorption performances and mechanisms. Bioresource Technology, 2021, 340, 125698.	9.6	106
78	Self-powered photoelectrochemical aptasensor based on phosphorus doped porous ultrathin g-C3N4 nanosheets enhanced by surface plasmon resonance effect. Biosensors and Bioelectronics, 2018, 121, 19-26.	10.1	104
79	Peroxymonosulfate activation of magnetic Co nanoparticles relative to an N-doped porous carbon under confinement: Boosting stability and performance. Separation and Purification Technology, 2020, 250, 117237.	7.9	103
80	Carbon-based core–shell nanostructured materials for electrochemical energy storage. Journal of Materials Chemistry A, 2018, 6, 7310-7337.	10.3	102
81	Metal-based quantum dots: synthesis, surface modification, transport and fate in aquatic environments and toxicity to microorganisms. RSC Advances, 2016, 6, 78595-78610.	3.6	101
82	Carbon felt cathodes for electro-Fenton process to remove tetracycline via synergistic adsorption and degradation. Science of the Total Environment, 2019, 670, 921-931.	8.0	99
83	Practical and regenerable electrochemical aptasensor based on nanoporous gold and thymine-Hg 2+ -thymine base pairs for Hg 2+ detection. Biosensors and Bioelectronics, 2017, 90, 542-548.	10.1	98
84	Novel insights into the adsorption of organic contaminants by biochar: A review. Chemosphere, 2022, 287, 132113.	8.2	97
85	Rapid adsorption of 2,4-dichlorophenoxyacetic acid by iron oxide nanoparticles-doped carboxylic ordered mesoporous carbon. Journal of Colloid and Interface Science, 2015, 445, 1-8.	9.4	93
86	Visible-light photocatalytic degradation of multiple antibiotics by AgI nanoparticle-sensitized Bi5O7I microspheres: Enhanced interfacial charge transfer based on Z-scheme heterojunctions. Journal of Catalysis, 2017, 352, 160-170.	6.2	92
87	Mechanistic insights into red mud, blast furnace slag, or metakaolin-assisted stabilization/solidification of arsenic-contaminated sediment. Environment International, 2019, 133, 105247.	10.0	91
88	Effective removal of Cr(<scp>vi</scp>) through adsorption and reduction by magnetic mesoporous carbon incorporated with polyaniline. RSC Advances, 2014, 4, 58362-58371.	3.6	90
89	Rapid reductive degradation of aqueous p-nitrophenol using nanoscale zero-valent iron particles immobilized on mesoporous silica with enhanced antioxidation effect. Applied Surface Science, 2015, 333, 220-228.	6.1	89
90	Application of abscisic acid and 6-benzylaminopurine modulated morpho-physiological and antioxidative defense responses of tomato (Solanum lycopersicum L.) by minimizing cobalt uptake. Chemosphere, 2021, 263, 128169.	8.2	88

#	Article	IF	CITATIONS
91	Enhanced visible light photocatalytic performance of polyaniline modified mesoporous single crystal TiO2 microsphere. Applied Surface Science, 2016, 387, 882-893.	6.1	87
92	Electron density modulation of Fe1-xCoxP nanosheet arrays by iron incorporation for highly efficient water splitting. Nano Energy, 2020, 67, 104174.	16.0	87
93	Synthesis of Pd/Au bimetallic nanoparticle-loaded ultrathin graphitic carbon nitride nanosheets for highly efficient catalytic reduction of p-nitrophenol. Journal of Colloid and Interface Science, 2017, 490, 834-843.	9.4	85
94	A tyrosinase biosensor based on ordered mesoporous carbon–Au/l-lysine/Au nanoparticles for simultaneous determination of hydroquinone and catechol. Analyst, The, 2013, 138, 3552.	3.5	82
95	Chiral pharmaceuticals: Environment sources, potential human health impacts, remediation technologies and future perspective. Environment International, 2018, 121, 523-537.	10.0	82
96	Population characteristics and influential factors of nitrogen cycling functional genes in heavy metal contaminated soil remediated by biochar and compost. Science of the Total Environment, 2019, 651, 2166-2174.	8.0	82
97	Bacterial-induced mineralization (BIM) for soil solidification and heavy metal stabilization: A critical review. Science of the Total Environment, 2020, 746, 140967.	8.0	82
98	Development of ozonation and reactive electrochemical membrane coupled process: Enhanced tetracycline mineralization and toxicity reduction. Chemical Engineering Journal, 2020, 383, 123149.	12.7	81
99	Current progress in degradation and removal methods of polybrominated diphenyl ethers from water and soil: A review. Journal of Hazardous Materials, 2021, 403, 123674.	12.4	79
100	Recent advances in the environmental applications of biosurfactant saponins: A review. Journal of Environmental Chemical Engineering, 2017, 5, 6030-6038.	6.7	78
101	Polyamide 6 microplastics facilitate methane production during anaerobic digestion of waste activated sludge. Chemical Engineering Journal, 2021, 408, 127251.	12.7	75
102	Hydrogen sulfide enhances rice tolerance to nickel through the prevention of chloroplast damage and the improvement of nitrogen metabolism under excessive nickel. Plant Physiology and Biochemistry, 2019, 138, 100-111.	5.8	73
103	Adsorption of agricultural wastewater contaminated with antibiotics, pesticides and toxic metals by functionalized magnetic nanoparticles. Journal of Environmental Chemical Engineering, 2018, 6, 6468-6478.	6.7	70
104	Insights into the oxidation of organic contaminants by iron nanoparticles encapsulated within boron and nitrogen co-doped carbon nanoshell: Catalyzed Fenton-like reaction at natural pH. Environment International, 2019, 128, 77-88.	10.0	70
105	Boron supply alleviates cadmium toxicity in rice (Oryza sativa L.) by enhancing cadmium adsorption on cell wall and triggering antioxidant defense system in roots. Chemosphere, 2021, 266, 128938.	8.2	68
106	Phosphorus-doped ordered mesoporous carbons embedded with Pd/Fe bimetal nanoparticles for the dechlorination of 2,4-dichlorophenol. Catalysis Science and Technology, 2016, 6, 1930-1939.	4.1	67
107	Magnetic MgFe2O4/biochar derived from pomelo peel as a persulfate activator for levofloxacin degradation: Effects and mechanistic consideration. Bioresource Technology, 2022, 346, 126547.	9.6	67
108	Effects of magnesium ferrite biochar on the cadmium passivation in acidic soil and bioavailability for packoi (Brassica chinensis L.). Journal of Environmental Management, 2019, 251, 109610.	7.8	65

#	Article	IF	CITATIONS
109	Attapulgite-supported nano-Fe0/peroxymonsulfate for quinclorac removal: Performance, mechanism and degradation pathway. Chemical Engineering Journal, 2019, 360, 104-114.	12.7	65
110	A review on percarbonate-based advanced oxidation processes for remediation of organic compounds in water. Environmental Research, 2021, 200, 111371.	7.5	65
111	CdS/Cu2S co-sensitized TiO2 branched nanorod arrays of enhanced photoelectrochemical properties by forming nanoscale heterostructure. Journal of Alloys and Compounds, 2016, 662, 516-527.	5.5	64
112	Label free detection of lead using impedimetric sensor based on ordered mesoporous carbon–gold nanoparticles and DNAzyme catalytic beacons. Talanta, 2016, 146, 641-647.	5.5	64
113	FellFelll layered double hydroxide modified carbon felt cathode for removal of ciprofloxacin in electro-Fenton process. Environmental Research, 2021, 197, 111144.	7.5	62
114	Recent advances in nitrous oxide production and mitigation in wastewater treatment. Water Research, 2020, 184, 116168.	11.3	61
115	Current progress in biosensors for organophosphorus pesticides based on enzyme functionalized nanostructures: a review. Analytical Methods, 2018, 10, 5468-5479.	2.7	59
116	Mitigation of acidogenic product inhibition and elevated mass transfer by biochar during anaerobic digestion of food waste. Bioresource Technology, 2021, 338, 125531.	9.6	59
117	Characteristics of denitrification genes and relevant enzyme activities in heavy-metal polluted soils remediated by biochar and compost. Science of the Total Environment, 2020, 739, 139987.	8.0	57
118	A reusable electrochemical biosensor for highly sensitive detection of mercury ions with an anionic intercalator supported on ordered mesoporous carbon/self-doped polyaniline nanofibers platform. Biochemical Engineering Journal, 2017, 117, 7-14.	3.6	56
119	Design and fabrication of exfoliated Mg/Al layered double hydroxides on biochar support. Journal of Cleaner Production, 2021, 289, 125142.	9.3	56
120	Remediation of cadmium-contaminated soils using Brassica napus: Effect of nitrogen fertilizers. Journal of Environmental Management, 2020, 255, 109885.	7.8	55
121	Effects of exogenous calcium and spermidine on cadmium stress moderation and metal accumulation in Boehmeria nivea (L.) Gaudich. Environmental Science and Pollution Research, 2016, 23, 8699-8708.	5.3	54
122	Aromatic organoarsenic compounds (AOCs) occurrence and remediation methods. Chemosphere, 2018, 207, 665-675.	8.2	54
123	Applications of nanoscale zero-valent iron and its composites to the removal of antibiotics: a review. Journal of Materials Science, 2019, 54, 12171-12188.	3.7	54
124	Ultrathin low dimensional heterostructure composites with superior photocatalytic activity: Insight into the multichannel charge transfer mechanism. Chemical Engineering Journal, 2020, 393, 124718.	12.7	54
125	γ-ray induced formation of oxygen vacancies and Ti3+ defects in anatase TiO2 for efficient photocatalytic organic pollutant degradation. Science of the Total Environment, 2020, 747, 141533.	8.0	53
126	Simultaneous removal of iron and manganese from acid mine drainage by acclimated bacteria. Journal of Hazardous Materials, 2020, 396, 122631.	12.4	53

#	Article	IF	CITATIONS
127	Three-dimensional MOF-derived hierarchically porous aerogels activate peroxymonosulfate for efficient organic pollutants removal. Chemical Engineering Journal, 2022, 427, 130830.	12.7	53
128	Cu-Doped Fe@Fe ₂ O ₃ core–shell nanoparticle shifted oxygen reduction pathway for high-efficiency arsenic removal in smelting wastewater. Environmental Science: Nano, 2018, 5, 1595-1607.	4.3	52
129	Silicon fertilizers, humic acid and their impact on physicochemical properties, availability and distribution of heavy metals in soil and soil aggregates. Science of the Total Environment, 2022, 822, 153483.	8.0	51
130	New insights into the activity of a biochar supported nanoscale zerovalent iron composite and nanoscale zero valent iron under anaerobic or aerobic conditions. RSC Advances, 2017, 7, 8755-8761.	3.6	50
131	Influence of roxithromycin as antibiotic residue on volatile fatty acids recovery in anaerobic fermentation of waste activated sludge. Journal of Hazardous Materials, 2020, 394, 122570.	12.4	50
132	Current progress in electrochemical anodic-oxidation of pharmaceuticals: Mechanisms, influencing factors, and new technique. Journal of Hazardous Materials, 2021, 418, 126313.	12.4	50
133	Simultaneous removal of atrazine and copper using polyacrylic acid-functionalized magnetic ordered mesoporous carbon from water: adsorption mechanism. Scientific Reports, 2017, 7, 43831.	3.3	49
134	Simultaneous degradation of p-arsanilic acid and inorganic arsenic removal using M-rGO/PS Fenton-like system under neutral conditions. Journal of Hazardous Materials, 2020, 399, 123032.	12.4	49
135	Combined removal of di(2-ethylhexyl)phthalate (DEHP) and Pb(<scp>ii</scp>) by using a cutinase loaded nanoporous gold-polyethyleneimine adsorbent. RSC Advances, 2014, 4, 55511-55518.	3.6	47
136	Key environmental factors to variation of ammonia-oxidizing archaea community and potential ammonia oxidation rate during agricultural waste composting. Bioresource Technology, 2018, 270, 278-285.	9.6	47
137	Effect of Fe2+, Mn2+ catalysts on the performance of electro-Fenton degradation of antibiotic ciprofloxacin, and expanding the utilizing of acid mine drainage. Science of the Total Environment, 2020, 720, 137560.	8.0	46
138	Application of Fourier transform ion cyclotron resonance mass spectrometry to characterize natural organic matter. Chemosphere, 2020, 260, 127458.	8.2	46
139	Manganese ferrite modified biochar from vinasse for enhanced adsorption of levofloxacin: Effects and mechanisms. Environmental Pollution, 2021, 272, 115968.	7.5	46
140	New insights into ball milling effects on MgAl-LDHs exfoliation on biochar support: A case study for cadmium adsorption. Journal of Hazardous Materials, 2021, 416, 126258.	12.4	46
141	Enhancing autotrophic nitrogen removal with a novel dissolved oxygen-differentiated airlift internal circulation reactor: Long-term operational performance and microbial characteristics. Journal of Environmental Management, 2021, 296, 113271.	7.8	46
142	Determination of Cd2+ and Pb2+ Based on Mesoporous Carbon Nitride/Self-Doped Polyaniline Nanofibers and Square Wave Anodic Stripping Voltammetry. Nanomaterials, 2016, 6, 7.	4.1	45
143	Effects of red mud based passivator on the transformation of Cd fraction in acidic Cd-polluted paddy soil and Cd absorption in rice. Science of the Total Environment, 2018, 640-641, 736-745.	8.0	45
144	Biohythane production and microbial characteristics of two alternating mesophilic and thermophilic two-stage anaerobic co-digesters fed with rice straw and pig manure. Bioresource Technology, 2021, 320, 124303.	9.6	45

#	Article	IF	CITATIONS
145	Optimization of flocculation conditions for soluble cadmium removal using the composite flocculant of green anion polyacrylamide and PAC by response surface methodology. Science of the Total Environment, 2018, 645, 267-276.	8.0	44
146	Ultrafine metal species confined in metal–organic frameworks: Fabrication, characterization and photocatalytic applications. Coordination Chemistry Reviews, 2021, 439, 213924.	18.8	42
147	Soil organic carbon and soil aggregate stability associated with aggregate fractions in a chronosequence of citrus orchards plantations. Journal of Environmental Management, 2021, 293, 112847.	7.8	41
148	Monitoring the nitrous oxide emissions and biological nutrient removal from wastewater treatment: Impact of perfluorooctanoic acid. Journal of Hazardous Materials, 2021, 402, 123469.	12.4	40
149	Responses of ammonia-oxidizing microorganisms to biochar and compost amendments of heavy metals-polluted soil. Journal of Environmental Sciences, 2021, 102, 263-272.	6.1	40
150	Current progress in treatment techniques of triclosan from wastewater: A review. Science of the Total Environment, 2019, 696, 133990.	8.0	39
151	Electrokinetic techniques, their enhancement techniques and composite techniques with other processes for persistent organic pollutants remediation in soil: A review. Journal of Industrial and Engineering Chemistry, 2021, 97, 163-172.	5.8	39
152	Formation and interdependence of disinfection byproducts during chlorination of natural organic matter in a conventional drinking water treatment plant. Chemosphere, 2020, 242, 125227.	8.2	38
153	Foliar application of Zn reduces Cd accumulation in grains of late rice by regulating the antioxidant system, enhancing Cd chelation onto cell wall of leaves, and inhibiting Cd translocation in rice. Science of the Total Environment, 2021, 770, 145302.	8.0	38
154	A novel modified Fe–Mn binary oxide graphite felt (FMBO-GF) cathode in a neutral electro-Fenton system for ciprofloxacin degradation. Environmental Pollution, 2021, 286, 117310.	7.5	38
155	Amplified and selective detection of manganese peroxidase genes based on enzyme-scaffolded-gold nanoclusters and mesoporous carbon nitride. Biosensors and Bioelectronics, 2015, 65, 382-389.	10.1	36
156	Comparisons of three plant species in accumulating polycyclic aromatic hydrocarbons (PAHs) from the atmosphere: a review. Environmental Science and Pollution Research, 2018, 25, 16548-16566.	5.3	36
157	Activation of persulfate with dual-doped reduced graphene oxide for degradation of alkylphenols. Chemical Engineering Journal, 2019, 376, 120891.	12.7	36
158	Structure-based synergistic mechanism for the degradation of typical antibiotics in electro-Fenton process using Pd–Fe3O4 model catalyst: Theoretical and experimental study. Journal of Catalysis, 2018, 365, 184-194.	6.2	35
159	Soil and fine roots ecological stoichiometry in different vegetation restoration stages in a karst area, southwest China. Journal of Environmental Management, 2019, 252, 109694.	7.8	35
160	Electrochemical treatments of coking wastewater and coal gasification wastewater with Ti/Ti4O7 and Ti/RuO2–lrO2 anodes. Journal of Environmental Management, 2020, 265, 110571.	7.8	35
161	A combined management scheme to simultaneously mitigate As and Cd concentrations in rice cultivated in contaminated paddy soil. Journal of Hazardous Materials, 2021, 416, 125837.	12.4	35
162	Research progress on the removal of hazardous perfluorochemicals: A review. Journal of Environmental Management, 2019, 250, 109488.	7.8	33

#	Article	IF	CITATIONS
163	The Use of Constructed Wetland for Mitigating Nitrogen and Phosphorus from Agricultural Runoff: A Review. Water (Switzerland), 2021, 13, 476.	2.7	33
164	Silicon-based additive on heavy metal remediation in soils: Toxicological effects, remediation techniques, and perspectives. Environmental Research, 2022, 205, 112244.	7.5	33
165	Sensitive impedimetric biosensor based on duplex-like DNA scaffolds and ordered mesoporous carbon nitride for silver(<scp>i</scp>) ion detection. Analyst, The, 2014, 139, 6529-6535.	3.5	32
166	Current Progress in Aptasensors for Heavy Metal Ions Based on Photoelectrochemical Method: A Review. Current Analytical Chemistry, 2018, 14, .	1.2	32
167	Geochemical fractionation of thallium in contaminated soils near a large-scale Hg-Tl mineralised area. Chemosphere, 2020, 239, 124775.	8.2	32
168	Degradation of several polycyclic aromatic hydrocarbons by laccase in reverse micelle system. Science of the Total Environment, 2020, 708, 134970.	8.0	32
169	Novel recycling of incinerated sewage sludge ash (ISSA) and waste bentonite as ceramsite for Pb-containing wastewater treatment: Performance and mechanism. Journal of Environmental Management, 2021, 288, 112382.	7.8	31
170	Removal of bisphenol A by iron nanoparticle-doped magnetic ordered mesoporous carbon. RSC Advances, 2016, 6, 25724-25732.	3.6	30
171	Activation of persulfate by stability-enhanced magnetic graphene oxide for the removal of 2,4-dichlorophenol. Science of the Total Environment, 2020, 707, 135656.	8.0	30
172	Applications and influencing factors of the biochar-persulfate based advanced oxidation processes for the remediation of groundwater and soil contaminated with organic compounds. Science of the Total Environment, 2022, 836, 155421.	8.0	30
173	Catalytic reduction of hexavalent chromium by a novel nitrogen-functionalized magnetic ordered mesoporous carbon doped with Pd nanoparticles. Environmental Science and Pollution Research, 2016, 23, 22027-22036.	5.3	29
174	The roles of suspended solids in persulfate/Fe2+ treatment of hydraulic fracturing wastewater: Synergistic interplay of inherent wastewater components. Chemical Engineering Journal, 2020, 388, 124243.	12.7	29
175	Ordered Mesoporous Carbon and Thiolated Polyaniline Modified Electrode for Simultaneous Determination of Cadmium(II) and Lead(II) by Anodic Stripping Voltammetry. Electroanalysis, 2014, 26, 2283-2291.	2.9	28
176	Effect of bismuth tungstate with different hierarchical architectures on photocatalytic degradation of norfloxacin under visible light. Transactions of Nonferrous Metals Society of China, 2017, 27, 1794-1803.	4.2	27
177	Input–output balance of cadmium in typical agriculture soils with historical sewage irrigation in China. Journal of Environmental Management, 2020, 276, 111298.	7.8	26
178	Thermochemical conversion of heavy metal contaminated biomass: Fate of the metals and their impact on products. Science of the Total Environment, 2022, 822, 153426.	8.0	26
179	Toward emerging applications using core–shell nanostructured materials: a review. Journal of Materials Science, 2022, 57, 10912-10942.	3.7	26
180	Spatial variation of sediment bacterial community in an acid mine drainage contaminated area and surrounding river basin. Journal of Environmental Management, 2019, 251, 109542.	7.8	25

#	Article	IF	CITATIONS
181	Concentrations and emissions of particulate matter and ammonia from extensive livestock farm in South China. Environmental Science and Pollution Research, 2019, 26, 1871-1879.	5.3	25
182	p-Arsanilic acid decontamination over a wide pH range using biochar-supported manganese ferrite material as an effective persulfate catalyst: Performances and mechanisms. Biochar, 2022, 4, .	12.6	23
183	Enhanced heterogeneous activation of persulfate by NixCo3–xO4 for oxidative degradation of tetracycline and bisphenol A. Journal of Environmental Chemical Engineering, 2020, 8, 104451.	6.7	22
184	The Fe3O4-modified biochar reduces arsenic availability in soil and arsenic accumulation in indica rice (Oryza sativa L.). Environmental Science and Pollution Research, 2021, 28, 18050-18061.	5.3	22
185	A novel biosensor for silver(<scp>i</scp>) ion detection based on nanoporous gold and duplex-like DNA scaffolds with anionic intercalator. RSC Advances, 2015, 5, 69738-69744.	3.6	21
186	Highly effective antibacterial activity by the synergistic effect of three dimensional ordered mesoporous carbon-lysozyme composite. Journal of Colloid and Interface Science, 2017, 503, 131-141.	9.4	19
187	Exploring the linkage between free nitrous acid accumulation and nitrous oxide emissions in a novel static/oxic/anoxic process. Bioresource Technology, 2020, 304, 123011.	9.6	19
188	Boron application mitigates Cd toxicity in leaves of rice by subcellular distribution, cell wall adsorption and antioxidant system. Ecotoxicology and Environmental Safety, 2021, 222, 112540.	6.0	19
189	Stimulation of pyrolytic carbon materials as electron shuttles on the anaerobic transformation of recalcitrant organic pollutants: A review. Science of the Total Environment, 2021, 801, 149696.	8.0	19
190	A label–free GR–5DNAzyme sensor for lead ions detection based on nanoporous gold and anionic intercalator. Talanta, 2017, 165, 274-281.	5.5	18
191	Performance and mechanism of As(III) removal from water using Fe-Al bimetallic material. Separation and Purification Technology, 2018, 191, 314-321.	7.9	17
192	Simultaneous remediation of methylene blue and Cr(VI) by mesoporous BiVO4 photocatalyst under visible-light illumination. Journal of the Taiwan Institute of Chemical Engineers, 2020, 112, 357-365.	5.3	17
193	Variations of disinfection byproduct precursors through conventional drinking water treatment processes and a real-time monitoring method. Chemosphere, 2021, 272, 129930.	8.2	17
194	Response of soil microbial communities to red mud-based stabilizer remediation of cadmium-contaminated farmland. Environmental Science and Pollution Research, 2018, 25, 11661-11669.	5.3	16
195	Synergistic utilization of inherent halides and alcohols in hydraulic fracturing wastewater for radical-based treatment: A case study of di-(2-ethylhexyl) phthalate removal. Journal of Hazardous Materials, 2020, 384, 121321.	12.4	16
196	Effect of Manure Compost on Distribution of Cu and Zn in Rhizosphere Soil and Heavy Metal Accumulation by Brassica juncea. Water, Air, and Soil Pollution, 2020, 231, 1.	2.4	16
197	Enhancing cadmium extraction potential of Brassica napus: Effect of rhizosphere interactions. Journal of Environmental Management, 2021, 284, 112056.	7.8	15
198	Effect of Pb(<scp>ii</scp>) on phenanthrene degradation by new isolated Bacillus sp. P1. RSC Advances, 2015, 5, 55812-55818.	3.6	14

#	Article	IF	CITATIONS
199	The study of a pilot-scale aerobic/Fenton/anoxic/aerobic process system for the treatment of landfill leachate. Environmental Technology (United Kingdom), 2018, 39, 1926-1936.	2.2	14
200	Characterization of Microcystis Aeruginosa immobilized in complex of PVA and sodium alginate and its application on phosphorous removal in wastewater. Journal of Central South University, 2015, 22, 95-102.	3.0	13
201	Enhancement of Fenton processes at initial circumneutral pH for the degradation of norfloxacin with Fe@Fe2O3 core-shell nanomaterials. Environmental Technology (United Kingdom), 2019, 40, 3632-3640.	2.2	12
202	Influence of chlortetracycline as an antibiotic residue on nitrous oxide emissions from wastewater treatment. Bioresource Technology, 2020, 313, 123696.	9.6	12
203	Triclosan facilitates the recovery of volatile fatty acids from waste activated sludge. Science of the Total Environment, 2021, 754, 142336.	8.0	12
204	Enzyme digestion combined with SP-ICP-MS analysis to characterize the bioaccumulation of gold nanoparticles by mustard and lettuce plants. Science of the Total Environment, 2021, 777, 146038.	8.0	12
205	Particulate pollution status and its characteristics during 2015–2016 in Hunan, China. Atmospheric Pollution Research, 2019, 10, 739-748.	3.8	11
206	Residual behavior and risk assessment of butralin in peanut fields. Environmental Monitoring and Assessment, 2020, 192, 62.	2.7	11
207	Elucidating the effects of TiO2 nanoparticles on the toxicity and accumulation of Cu in soybean plants (Glycine max L.). Ecotoxicology and Environmental Safety, 2021, 219, 112312.	6.0	11
208	Exploring the role of Fe species from biochar-iron composites in the removal and long-term immobilization of SeO42- against competing oxyanions. Journal of Hazardous Materials, 2021, 418, 126311.	12.4	11
209	Formation of composite sorbent by P. chrysogenum strain F1 and ferrihydrite in water for arsenic removal. International Biodeterioration and Biodegradation, 2018, 132, 208-215.	3.9	10
210	Detection of C60 in environmental water using dispersive liquid–liquid micro-extraction followed by high-performance liquid chromatography. Environmental Technology (United Kingdom), 2020, 41, 1015-1022.	2.2	10
211	Effectiveness and limitation of A-nZVI for restoration of a highly As-contaminated soil. Journal of Cleaner Production, 2021, 284, 124691.	9.3	9
212	Distribution and migration characteristics of dinitrotoluene sulfonates (DNTs) in typical TNT production sites: Effects and health risk assessment. Journal of Environmental Management, 2021, 287, 112342.	7.8	9
213	High-efficiency degradation of p-arsanilic acid and arsenic immobilization with iron encapsulated B/N-doped carbon nanotubes at natural solution pH. Science of the Total Environment, 2021, 785, 147152.	8.0	9
214	Benzotriazole Ultraviolet Stabilizers Promote Breast Cancer Cell Proliferation via Activating Estrogen-Related Receptors α and γ at Human-Relevant Levels. Environmental Science & Technology, 2022, 56, 2466-2475.	10.0	9
215	Disinfection techniques of human norovirus in municipal wastewater: Challenges and future perspectives. Current Opinion in Environmental Science and Health, 2020, 17, 29-34.	4.1	8
216	Efficient Removal of Antimony(III) in Aqueous Phase by Nano-Fe3O4 Modified High-Iron Red Mud: Study on Its Performance and Mechanism. Water (Switzerland), 2021, 13, 809.	2.7	8

#	Article	IF	CITATIONS
217	Characteristics and Influencing Factors of Microbial Community in Heavy Metal Contaminated Soil under Silicon Fertilizer and Biochar Remediation. Adsorption Science and Technology, 2021, 2021, .	3.2	8
218	Editorial of the VSI "Environmental, ecological and public health considerations regarding coronaviruses, other viruses, and other microorganisms potentially causing pandemic diseases― Environmental Research, 2021, 192, 110322.	7.5	7
219	Efficient removal of pefloxacin from aqueous solution by acid–alkali modified sludge-based biochar: adsorption kinetics, isotherm, thermodynamics, and mechanism. Environmental Science and Pollution Research, 2022, 29, 43201-43211.	5.3	7
220	Editorial of the VSI "Antibiotics and heavy metals in the environment: Facing the challenge― Science of the Total Environment, 2019, 678, 30-32.	8.0	6
221	Interaction of tetramer protein with carbon nanotubes. Applied Surface Science, 2019, 464, 30-35.	6.1	6
222	Enhanced degradation of 1-naphthol in landfill leachate using <i>Arthrobacter</i> sp Environmental Technology (United Kingdom), 2019, 40, 835-842.	2.2	6
223	Effect of RM-based-passivator for the remediation of two kinds of Cd polluted paddy soils and mechanism of Cd(II) adsorption. Environmental Technology (United Kingdom), 2021, 42, 1623-1633.	2.2	5
224	Magnetic biochar-based composites for removal of recalcitrant pollutants in water. , 2021, , 163-187.		5
225	A Novel Manganese-Rich Pokeweed Biochar for Highly Efficient Adsorption of Heavy Metals from Wastewater: Performance, Mechanisms, and Potential Risk Analysis. Processes, 2021, 9, 1209.	2.8	5
226	Vinasse-based biochar magnetic composites: adsorptive removal of tetracycline in aqueous solutions. Environmental Science and Pollution Research, 2023, 30, 8916-8927.	5.3	5
227	Time-dependent antioxidative responses of ramie (Boehmeria nivea (L.) Gaudich) to moderate cadmium stress and its up-regulation mechanism by spermidine antioxidant. RSC Advances, 2015, 5, 76141-76149.	3.6	4
228	Mesoporous Carbon-Based Composites for Adsorption of Heavy Metals. , 2019, , 63-102.		4
229	Editorial: New Research on Soil Degradation and Restoration. Journal of Environmental Management, 2020, 269, 110851.	7.8	4
230	Iron-based materials for removal of arsenic from water. , 2021, , 209-245.		4
231	Voltammetric Biosensor Based on Nitrogen-doped Ordered Mesoporous Carbon for Detection of Organophosphorus Pesticides in Vegetables. Current Analytical Chemistry, 2018, 15, 92-100.	1.2	4
232	Response to comment on "Chiral pharmaceuticals: Environment sources, potential human health impacts, remediation technologies and future perspective― Environment International, 2019, 127, 1-4.	10.0	3
233	Response to the comments on "peroxydisulfate chemistry in the environmental literature: A brief critique''. Journal of Hazardous Materials, 2019, 367, 356.	12.4	3
234	New research on water, waste and energy management, with special focus on antibiotics and priority pollutants. Environmental Research, 2021, 201, 111582.	7.5	3

#	Article	IF	CITATIONS
235	New research on reduction and/or elimination of hazardous substances in the design, manufacture and application of chemical products. Environmental Research, 2021, 201, 111601.	7.5	3
236	Study on Magnetic Chitosan Microparticles for Rapid Removal of Heavy Metals. Advanced Materials Research, 2012, 518-523, 2844-2848.	0.3	2
237	Nanoporous Materials Based Sensors for Pollutant Detection. , 2019, , 265-291.		2
238	Mesoporous Carbon Based Composites for Removal of Recalcitrant Pollutants From Water. , 2019, , 31-61.		1
239	Dissipation Behavior and Residue Distribution of Famoxadone and Cymoxanil in Cucumber and Soil Ecosystem Under Open-Field Conditions. Water, Air, and Soil Pollution, 2020, 231, 1.	2.4	1
240	Determination of Lignocellulase Activity and Gene Expression Using Magnetic Nanoparticle-Based Electrochemical Biosensor. Advanced Materials Research, 0, 518-523, 309-313.	0.3	0
241	Enhancement of Fenton processes at initial circumneutral pH for the degradation of norfloxacin with Fe@FeS core-shell nanowires. Environmental Technology (United Kingdom), 2022, , 1-24.	2.2	Ο
242	Current Progress of Microplastics in Sewage Sludge. Handbook of Environmental Chemistry, 2022, , 1.	0.4	0
243	Biochars' potential role in the remediation, revegetation, and restoration of contaminated soils. , 2022, , 381-399.		0